PHYSICAL REVIEW B **79**, 180403(R) (2009)

Systematics of electromagnons in the spiral spin-ordered states of $R\mathrm{MnO_3}$

J. S. Lee,[1,*] N. Kida,[1] S. Miyahara,[1] Y. Takahashi,[1] Y. Yamasaki,[2] R. Shimano,[1,3] N. Furukawa,[1,4] and Y. Tokura[1,2,5]

[1]*Department of Applied Physics, Multiferroics Project, Exploratory Research for Advanced Technology (ERATO), Japan Science and Technology Agency (JST), University of Tokyo, Tokyo 113-8656, Japan*

[2]*Department of Applied Physics, University of Tokyo, Tokyo 113-8656, Japan*

[3]*Department of Physics, The University of Tokyo, Tokyo 113-0033, Japan*

[4]*Department of Physics and Mathematics, Aoyama Gakuin University, Sagamihara, Kanagawa 229-8558, Japan*

[5]*Cross-Correlated Materials Research Group (CMRG), ASI, RIKEN, Wako, Saitama 351-0198, Japan*

(Received 28 February 2009; revised manuscript received 20 April 2009; published 7 May 2009)

Electromagnon, magnetic excitation driven by an electric field of light, has been investigated for a series of perovskite manganites $R\mathrm{MnO_3}$. Two distinct excitations commonly appear in the spiral spin-ordered state, and systematic changes in their peak positions and spectral weights were observed as a function of the radius of the *R*-ion or equivalently of spin-exchange interaction energies. By comparing the results with the spin-wave calculation based on the Heisenberg model, the higher-lying excitation is assigned to the zone-edge magnon. The strong electric-dipole activity of these magnetic excitations is discussed in terms of dynamic coupling among the collective modes.

DOI: 10.1103/PhysRevB.79.180403 PACS number(s): 75.47.Lx, 75.80.+q, 76.50.+g, 78.30.−j

When lattice or electronic degrees of freedom show the long-range order in a solid, each or combination of them can host the corresponding collective excitation; one such example is a magnon, a spin excitation excited by an oscillating magnetic field. Recently, the so-called electromagnon, excited by a light electric field and not by a magnetic field, has been attracting great interest. Although its existence was predicted already in the 1960s,[1] it was just recently that the electromagnon with a large electric-dipole strength was experimentally observed in the perovskite manganites $R\mathrm{MnO_3}$ with R=Tb and Gd.[2] These compounds are the so-called multiferroics where the magnetic and the ferroelectric (FE) orders coexist,[3,4] and the spontaneous polarization (P_s) in the FE state arises from the Dzyaloshinskii-Moriya interaction.[5–7] The same interaction has been considered to explain the mechanism of the electromagnons,[8,9] e.g., a rotation mode of the spiral spin plane inducing an electric-dipole moment along the plane.[8] A collection of experimental results, however, revealed that such a model could not explain the light-polarization dependence of the excitation. For example, as the spiral spin plane changes from the *bc* to the *ab* plane, the P_s direction changes from the *c* axis to the *a* axis consistently with the theoretical prediction,[5,8] but the electromagnons remain active only along the *a* axis.[10–13] Instead, different scenarios have been proposed to explain such light-polarization dependence of the electromagnon by assigning the excitation to a two-magnon continuum[10,11,13,14] or to one magnon,[15,16] both can gain electric-dipole activity through the Heisenberg coupling between the spins.

In this Rapid Communication, we have investigated the electromagnetic response in the terahertz (THz) region of a series of $R\mathrm{MnO_3}$ with R=Gd, Tb, Dy, and mixtures of them. As the size of the *R* ions becomes smaller, the crystal structure is more distorted which will change the spin-exchange energies and modify the properties of magnetic excitations accordingly. As a function of spin-exchange interaction energies, we observed the systematic evolution of the electromagnon in its spectral shape, resonance energy, and spectral weight (SW). Combining these experimental findings and the spin-wave calculation based on the Heisenberg model, we could clearly elucidate the character of the electromagnons and discuss the origin of their strong electric-dipole activity.

Single crystals were grown by a floating zone method.[3] We performed the transmission experiment using THz time-domain spectroscopy below 10 meV,[11] and the transmission and the reflection experiments using Fourier-transform spectroscopy above 4 meV, and determined complex optical constants unambiguously. In the following, we deal with the real part of the optical conductivity, $\sigma_1(\omega)$, as the contribution of the magnetic permeability is negligible in the measured energy range.[11,13]

Let us first examine the optical conductivity spectra of $\mathrm{Gd_{0.7}Tb_{0.3}MnO_3}$ as the prototypical example which has plentiful magnetic/electric phases as a function of temperature (T) (Ref. 17): (i) paramagnetic/paraelectric state at $T>42$ K, (ii) collinear spin-order/paraelectric state at $24<T<42$ K, (iii) *ab*-spiral spin-order/ferroelectric state at $14<T<24$ K, and (iv) *A*-type antiferromagnetic (*A*-AFM)/paraelectric state at $T<14$ K. In the paramagnetic/paraelectric state, e.g., at 200 K, the optical spectra in this energy range, shown in Fig. 1(a), have a single contribution around 14 meV, which is ascribed to an infrared-active optical phonon. In the spiral spin-ordered state (16 K), however, three additional peaks appear around 3, 9, and 17 meV. In the *A*-AFM state, the two lower-energy peaks among them disappear [a black curve in the inset of Fig. 1(a)], whereas the higher-energy peak still remains together with the phonon. This suggests that the highest-energy peak has a different origin compared to the other two lower-energy peaks. The same figure shows also the optical response of $\mathrm{GdMnO_3}$ at 15 K. While this compound is in the *A*-AFM state such as $\mathrm{Gd_{0.7}Tb_{0.3}MnO_3}$ at 10 K,[4] its $\sigma_1(\omega)$ has a contribution only from the phonon around 14 meV. Such a difference between $\mathrm{Gd_{0.7}Tb_{0.3}MnO_3}$ and $\mathrm{GdMnO_3}$ clearly indicates that the peak around 17 meV should be related to the Tb ion rather than to the Mn ion. From here on, we focus on two lower-energy peaks located below the lowest-lying phonon as the excitations contributed to by the Mn ion.

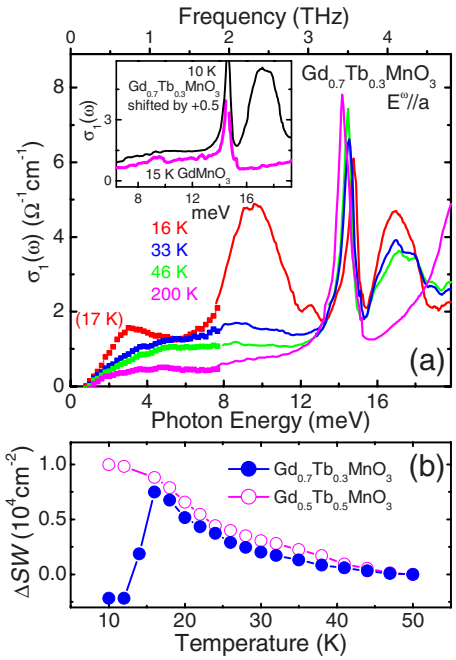

FIG. 1. (Color online) (a) The optical conductivity spectra $\sigma_1(\omega)$ below 20 meV of $Gd_{0.7}Tb_{0.3}MnO_3$ along the a axis. The results displayed with the symbols (below ~8 meV) are taken from Ref. 13. The inset shows $\sigma_1(\omega)$ of $Gd_{0.7}Tb_{0.3}MnO_3$ at 10 K and of $GdMnO_3$ at 15 K, both of which are in the A-AFM state. (b) Temperature-dependent spectral weight of the electromagnons obtained by integrating $\sigma_1(\omega)$ up to 12.5 meV.

Figure 1(b) shows the temperature-dependent SW of the magnetic excitations for $Gd_{0.7}Tb_{0.3}MnO_3$ obtained by integrating $\sigma_1(\omega)$; $SW(T)=\int_0^{12.5\ \mathrm{meV}}\sigma_1(\omega)d\omega$ and $\Delta SW(T)=SW(T)-SW(50\ \mathrm{K})$. It shows a gradual increase with successive magnetic transitions below 42 K and a sudden drop on entering the A-AFM state, which implies the magnetic origin of these excitations. The same figure shows a similar behavior of ΔSW for $Gd_{0.5}Tb_{0.5}MnO_3$ which keeps increasing down to 10 K in the spiral spin-ordered state. [As shown in Figs. 2(a) and 2(b), their spectral shapes are also similar.] Considering that two compounds have different spiral planes, i.e., the ab and bc plane for $Gd_{0.7}Tb_{0.3}MnO_3$ and for $Gd_{0.5}Tb_{0.5}MnO_3$, respectively,[17] such similar behaviors of electric-dipole active magnetic excitations demonstrate that their origin should be related to the symmetric exchange term proportional to the inner product of the neighboring spin moments, which is common for the ab- and bc-spiral states.

Figure 2 shows the optical conductivity spectra for a series of RMnO$_3$ at 16 (17) K for $R=Gd_{0.7}Tb_{0.3}$ and at 10 K for the others. At the corresponding temperatures the $R=Gd_{0.7}Tb_{0.3}$ compound is in the ab-spiral spin-order state, whereas the others are in the bc-spiral state. All the spectra have the common spectral features in this energy range, i.e., two peaks around 1 and 2 THz, which are here termed as modes A and B, respectively. For $R=Gd_{0.7}Tb_{0.3}$, these peaks are well separated and mode B is much stronger than mode A. For R=Dy, however, mode B is located close to mode A and their spectral weights are comparable with each other.

For the more quantitative analysis, we estimated the energy position and the spectral weight of each peak and displayed them in Figs. 3(a) and 3(b), respectively, as a function of the radius of the R ion. The peak positions were determined from the energy values where the $\sigma_1(\omega)$ is at maximum. As the radius of the R ion becomes smaller, mode B shows a remarkable shift from 9.5 meV for $R=Gd_{0.7}Tb_{0.3}$ to about 5 meV for R=Dy. Such a peak shift is less pronounced for mode A. In estimating the spectral weight by the integration of $\sigma_1(\omega)$, the contribution of each peak was decomposed by the frequencies where the $\sigma_1(\omega)$ take the minima, e.g., for $R=Gd_{0.5}Tb_{0.5}$ the regions of 0–5.3 and 5.3–12.5 meV for modes A and B, respectively. With decreasing the radius of the R ion, the spectral weight of mode A increases and that of mode B decreases, whereas the total summation of them exhibits only a minor reduction.

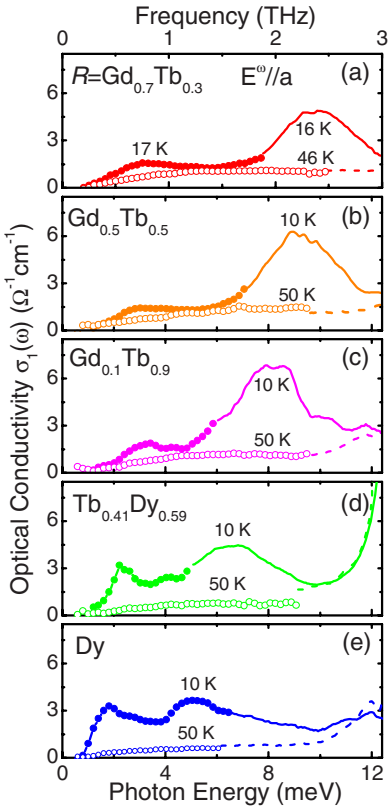

FIG. 2. (Color online) The optical conductivity spectra $\sigma_1(\omega)$ of RMnO$_3$ in the spiral spin (ferroelectric) state and the paramagnetic/paraelectric state for (a) $R=Gd_{0.7}Tb_{0.3}$, (b) $Gd_{0.5}Tb_{0.5}$, (c) $Gd_{0.1}Tb_{0.9}$, (d) $Tb_{0.41}Dy_{0.59}$, and (e) Dy. In each curve, the symbols correspond to the results obtained by THz time-domain spectroscopy and the solid and dashed lines by Fourier-transform spectroscopy. The results displayed with the symbols for $R=Gd_{0.7}Tb_{0.3}$ are taken from Ref. 13.

Since the collective excitation discussed here is magnetic in nature, we examine how magnetic excitations evolve in these materials. The magnetic features of RMnO$_3$ can be described by Heisenberg model with the nearest-neighbor ferromagnetic interactions in the ab-plane J_{ab} and antiferromagnetic ones along the c-axis J_c, and also by the next-nearest-neighbor antiferromagnetic exchange J_b along the b axis [Fig. 4(a)].[18] Using the superexchange formulation in Ref. 19, J_{ab} and J_c were calculated with structural parameters

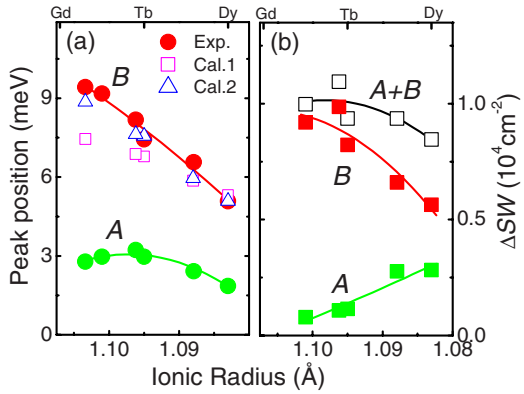

FIG. 3. (Color online) (a) Peak positions of the electromagnons (modes A and B) as a function of the radius of the R ions. Open symbols are zone-edge magnon energies as the energy of mode B obtained by the spin-wave theory using two sets of exchange energies; parameters for Cal.1 (Cal.2) are shown by open (closed) symbols in Fig. 4(b). (b) SW of the electromagnon; the respective SW for modes A and B and their total sum. The values are the differences between the SWs at 10 and 50 K. The result for $R=Gd_{0.7}Tb_{0.3}$ is omitted since the lowest temperature for the available data is 16 K, which is rather high compared to 10 K considering the strong temperature dependence of the spectral weight. The solid lines are merely guides for the eyes.

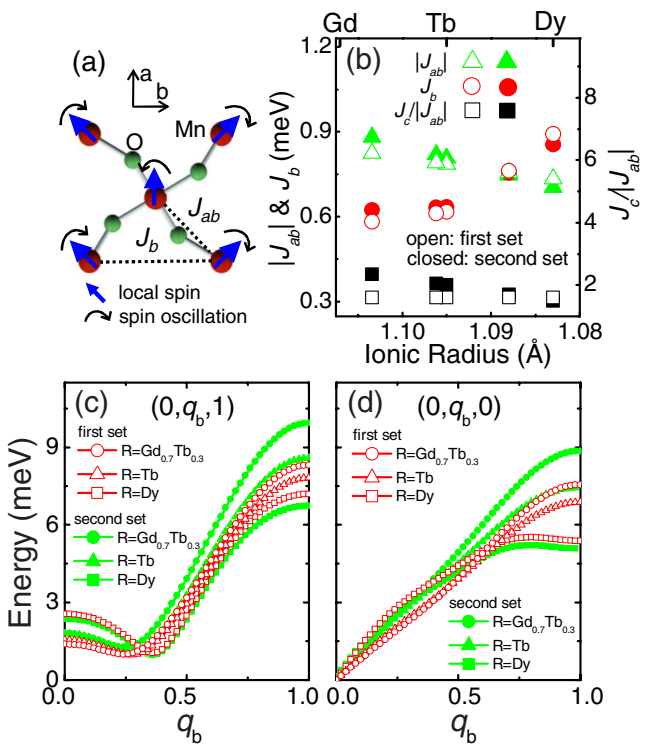

FIG. 4. (Color online) (a) Sketch of the crystal structure of $RMnO_3$ in the ab plane with R ion omitted. Exchange energies of J_{ab} (ferromagnetic) and J_b (antiferromagnetic) are indicated. The arrows correspond to the local spins and their oscillations with an excitation of the magnon at $q=(0,1,0)$. (b) $|J_{ab}|$, J_b, and $J_c/|J_{ab}|$ as a function of the radius of the R ions. The open symbols correspond to the first parameter set obtained by using structural data reported by Alonso *et al.* (Ref. 20), and closed symbols correspond to the second set estimated to reproduce the neutron scattering and the magnetic-resonance experiments (Ref. 16). [(c) and (d)] Magnon dispersions along the b axis with the parameters corresponding to $R=Gd_{0.7}Tb_{0.3}$, Tb, and Dy.

reported by Alonso *et al.*[20] For the intermediate compounds, of which structural data are not available, J_{ab} are estimated by a linear interpolation of the structural parameters and $J_c/|J_{ab}|$ is assumed as ~ 1.6 [Fig. 4(b)]. Frustration between J_{ab} and J_c leads to the spiral spin order with a modulation vector $q_m=1/(2\pi)\cos^{-1}(|J_{ab}|/2J_b)$,[18] which could be determined experimentally[3,4,17,18] and used to estimate the J_b values as shown in Fig. 4(b). By using these values and assuming the single-ion anisotropy energy $\Lambda=0.2|J_{ab}|$, we obtained the magnon dispersion curve as shown in Figs. 4(c) and 4(d). The dispersion along $q=(0,q_b,1)$ has a minimum at a finite q_b, which corresponds to the magnetic modulation vector.[3,21] As the involved exchange energies vary, the magnon at the zone edge, i.e., at $q=(0,1,0)$, exhibits a noticeable energy shift compared to magnons at other q values.

For the perovskite manganites, the symmetric spin-exchange term can induce the local electric-dipole moment, proportional to the inner product of the neighboring spin moments, but its net contribution is zero owing to the symmetry.[16] Nevertheless, the excitation of the zone-edge magnon at $q=(0,1,0)$, corresponding to the staggered rotation of the local spins as indicated by the arrows in Fig. 4(a), can induce a uniform modulation of the local dipole moment along the a axis irrespective of the spiral spin plane, leading to the coupling with light electric field along the same direction,[16] or possibly mediated by the phonons.[15] As shown with open squares in Fig. 3(a), the energy position of this zone-edge magnon and its shift as a function of the radius of the R ion are comparable with those of mode B. This leads us to conclude that mode B correspond to the zone-edge electromagnon induced by symmetric spin-dependent polarizations.

While the comparison between the energies of mode B and the zone-edge magnon shows a fairly good agreement between them, the peak position observed for the large R ions is noticeably larger than the calculation. In order to have a better fitting, we re-estimate spin-exchange energies, which are shown with closed symbols in Fig. 4(b). For $R=$Tb and Dy, the parameters were determined to reproduce the magnon dispersion and the magnon frequencies for each compound,[11,21] as discussed in detail elsewhere.[16] For the others, the values are obtained by a linear interpolation. As shown in Fig. 3(a), the model calculation using this second set of parameters could reproduce systematic peak shift of the electromagnon quite well. Conversely, this clearly supports the assignment of the electromagnon around 2 THz (mode B) to the zone-edge magnon. Comparing the energies of mode A and the magnons, mode A should correspond to the magnons near the zone center, although it is not clear which q value and magnon branch are responsible for that.

Another important spectral feature in these series compounds is the systematic change in the SW; with the decrease in the ionic radius, the SW of mode B decreases whereas that of mode A increases. [See Figs. 2 and 3(b).] Such an opposite trend of SW suggests that the origin of the electric-dipole

activity of each excitation should be different. Since such spectral changes occur together with a large peak shift, it would be worthwhile to examine the possibility of the hybridization effects among the modes which can be coupled with each other.

The excitation of the zone-edge magnon ($q_b=1$) accompanies the modulation of the exchange energy along the b direction which resembles the one induced by the infrared-active phonons along the a axis.[15,16] Therefore, the coupling between them can be expected. Given such coupling and the SW transfer from the phonons to the electromagnon,[9,10,14] the larger energy separation between them by a redshift of the electromagnon can lead to the weakening of the hybridization which can be partly responsible for the smaller SW of mode B for R=Dy. For mode A, since the enhancement of its SW accompanies the redshift of the peak, a different approach should be applied. Instead of the coupling with the phonons, one can assume the hybridization between the electromagnons themselves, which may be allowed by a magnetic anisotropy in the spiral spin-order state.[15,16] The smaller energy separation between modes A and B for the compounds with the smaller R ions will promote their hybridization and lead to the SW increase (decrease) of mode A (B). Note that this discussion about the hybridization effects assumed that the matrix element would not change so much depending on the compounds with different R ions. A more elaborate theoretical approach including all such aspects is necessary to explain systematic changes in the spectral weights of the electromagnons.

In summary, we have investigated the electromagnon excitations located at about 1 and 2 THz in a series of the perovskite manganites RMnO$_3$. With a variation in the radius of the R ions, we observed a large and systematic change in the peak position of the higher-energy electromagnon and could successfully explain it by assigning the excitation to the zone-edge magnon. Concerning the lower-energy electromagnon which arises from the magnons near the magnetic zone center, our experimental results suggest that the origin of its dipole activity should be different from that of the zone-edge electromagnon. Whereas the zone-edge electromagnon could have a dipole activity from strong coupling with phonons, the lower-energy electromagnon would gain a dipole strength from the coupling with the higher-lying zone-edge electromagnon.

We thank M. Mochizuki for fruitful discussion. This work was in part supported by Grant-In-Aids for Scientific Research (Grants No. 16076205 and No. 20340086) from the Ministry of Education, Culture, Sports and Technology (MEXT), Japan.

*jslee@erato-mf.t.u-tokyo.ac.jp

[1] V. G. Bar'yakhtar and I. E. Chupis, Fiz. Tverd. Tela (Leningrad) **11**, 3242 (1969) [Sov. Phys. Solid State **11**, 2628 (1970)].
[2] A. Pimenov, A. A. Mukhin, V. Yu. Ivanov, V. D. Travkin, A. M. Balbashov, and A. Loidl, Nat. Phys. **2**, 97 (2006).
[3] T. Kimura, T. Goto, H. Shintani, K. Ishizaka, T. Arima, and Y. Tokura, Nature (London) **426**, 55 (2003).
[4] T. Goto, T. Kimura, G. Lawes, A. P. Ramirez, and Y. Tokura, Phys. Rev. Lett. **92**, 257201 (2004).
[5] H. Katsura, N. Nagaosa, and A. V. Balatsky, Phys. Rev. Lett. **95**, 057205 (2005).
[6] I. A. Sergienko and E. Dagotto, Phys. Rev. B **73**, 094434 (2006).
[7] M. Mostovoy, Phys. Rev. Lett. **96**, 067601 (2006).
[8] H. Katsura, A. V. Balatsky, and N. Nagaosa, Phys. Rev. Lett. **98**, 027203 (2007).
[9] A. Pimenov, T. Rudolf, F. Mayr, A. Loidl, A. A. Mukhin, and A. M. Balbashov, Phys. Rev. B **74**, 100403(R) (2006).
[10] R. Valdés Aguilar, A. B. Sushkov, C. L. Zhang, Y. J. Choi, S.-W. Cheong, and H. D. Drew, Phys. Rev. B **76**, 060404(R) (2007).
[11] N. Kida, Y. Ikebe, Y. Takahashi, J. P. He, Y. Kaneko, Y. Yamasaki, R. Shimano, T. Arima, N. Nagaosa, and Y. Tokura, Phys. Rev. B **78**, 104414 (2008).
[12] A. Pimenov, A. Loidl, A. A. Mukhin, V. D. Travkin, V. Y. Ivanov, and A. M. Balbashov, Phys. Rev. B **77**, 014438 (2008).
[13] N. Kida, Y. Yamasaki, R. Shimano, T.-h. Arima, and Y. Tokura, J. Phys. Soc. Jpn. **77**, 123704 (2008).
[14] Y. Takahashi, N. Kida, Y. Yamasaki, J. Fujioka, T. Arima, R. Shimano, S. Miyahara, M. Mochizuki, N. Furukawa, and Y. Tokura, Phys. Rev. Lett. **101**, 187201 (2008).
[15] R. Valdés Aguilar, M. Mostovoy, A. B. Sushkov, C. L. Zhang, Y. J. Choi, S.-W. Cheong, and H. D. Drew, Phys. Rev. Lett. **102**, 047203 (2009).
[16] S. Miyahara and N. Furukawa, arXiv:0811.4082 (unpublished).
[17] Y. Yamasaki, H. Sagayama, N. Abe, T. Arima, K. Sasai, M. Matsuura, K. Hirota, D. Okuyama, Y. Noda, and Y. Tokura, Phys. Rev. Lett. **101**, 097204 (2008).
[18] T. Kimura, S. Ishihara, H. Shintani, T. Arima, K. T. Takahashi, K. Ishizaka, and Y. Tokura, Phys. Rev. B **68**, 060403(R) (2003).
[19] L. E. Gontchar and A. E. Nikiforov, Phys. Rev. B **66**, 014437 (2002).
[20] J. A. Alonso, M. J. Martinez-Lope, M. T. Casais, and M. T. Fernández-Díaz, Inorg. Chem. **39**, 917 (2000).
[21] D. Senff, P. Link, K. Hradil, A. Hiess, L. P. Regnault, Y. Sidis, N. Aliouane, D. N. Argyriou, and M. Braden, Phys. Rev. Lett. **98**, 137206 (2007).